Journal of Biomedical Optics

SPIEDigitalLibrary.org/jbo

Endomicroscopy imaging of epithelial structures using tissue autofluorescence

Bevin Lin
Shiro Urayama
Ramez M. G. Saroufeem
Dennis L. Matthews
Stavros G. Demos

SPIE

Endomicroscopy imaging of epithelial structures using tissue autofluorescence

Bevin Lin,[a,b] Shiro Urayama,[c] Ramez M. G. Saroufeem,[d] Dennis L. Matthews,[a,b] and Stavros G. Demos[a,e]
[a]University of California, Davis, NSF Center for Biophotonics Science & Technology, 4800 2nd Avenue, Sacramento, California 95817
[b]University of California, Davis, Department of Biomedical Engineering, One Shields Avenue, Davis, California 95616
[c]University of California, Davis Medical Center, Division of Gastroenterology and Hepatology, 4150 V Street, Suite 3500, Sacramento, California 95817
[d]University of California, Davis Medical Center, Department of Pathology, 4400 V Street, Sacramento, California 95817
[e]Lawrence Livermore National Laboratory, 7000 East Avenue, Livermore, California 94550

Abstract. We explore autofluorescence endomicroscopy as a potential tool for real-time visualization of epithelial tissue microstructure and organization in a clinical setting. The design parameters are explored using two experimental systems—an Olympus Medical Systems Corp. stand-alone clinical prototype probe, and a custom built bench-top rigid fiber conduit prototype. Both systems entail ultraviolet excitation at 266 nm and/or 325 nm using compact laser sources. Preliminary results using *ex vivo* animal and human tissue specimens suggest that this technology can be translated toward *in vivo* application to address the need for real-time histology.
 [DOI: 10.1117/1.3565216]

Keywords: endomicroscopy; ultraviolet autofluorescence; real-time histology.

Paper 10348RR received Jun. 23, 2010; revised manuscript received Feb. 21, 2011; accepted for publication Feb. 22, 2011; published online Apr. 18, 2011.

1 Introduction

Late stage cancers visible at the tissue level are very difficult to treat. The current gold standard for histopathological diagnosis involves removal of tissue and lengthy preparation of biopsy specimens.[1] This often hinders the delivery of optimal and timely medical care in many of the patients. It is believed that a critical component to future medical imaging would include techniques that provide diagnosis of early stage disease and imaging of abnormal cellular development *in vivo*. A number of endomicroscopy techniques that provide real-time imaging of tissue microstructures have emerged in recent years, accompanied by methods to generate contrast between cellular components. Optical coherence tomography provides images of major structural components of the mucosa and submucosa at higher resolution than catheter probe endoscopic ultrasound,[2] allowing visibility of normal squamous mucosa and specialized intestinal metaplasia in the esophagus, but has not yet been shown to adequately differentiate between dysplastic and intramucosal carcinoma.[3] Magnification chromoendoscopy includes topical application of contrast agents such as indigo carmine and acetic acid and has shown to be feasible and safe, although several limitations have prevented widespread use.[4] In addition, a number of studies have explored white light (WL) endomicroscopy in combination with topical application of contrast agents such as methylene blue[5] or acriflavine hydrochloride.[6] Clinical studies employing confocal endomicroscopy in conjunction with the use of intravenous fluorescein or indocyanine green as contrast agents are currently in progress. The confocal system is either integrated into the distal tip of a conventional upper endoscope, or is inserted through the accessory channel of a traditional endoscope.[7,8] Two FDA-approved confocal endomicroscopy systems manufactured by Pentax Corporation[9–11] and Mauna Kea Technologies[12,13] are currently available. While *in vivo* cellular imaging was successfully achieved, the image quality depends on contrast agent concentration and uptake, leakage, pattern distortion, and other complications directly related to intravenous administration, including rare but serious adverse events.[14]

Acquisition of diagnostic images without the use of contrast agents would arguably reduce cost and improve time efficiency in the operating room. Reflectance confocal endomicroscopy achieves a high degree of functionality,[15–17] but typically requires a tissue preparation step to enhance visualization of the cell nuclei. Nonlinear techniques such as two photon autofluorescence microscopy use native tissue contrast mechanism[18,19] but implementation in a clinical environment requires accommodation of complex instrumentation. Olympus Medical Systems Corp. has developed a magnification high-resolution endoscopy system[20,21] providing an increased sensitivity in detection of mucosal and vascular patterns without the use of contrast agents by implementing WL and narrowband imaging, but it does not provide imaging at the cellular level.

Imaging tissue structures at the cellular level using intrinsic contrast mechanisms, such as autofluorescence (AF), requires the optimization of multiple parameters that govern image formation. These include optimization of the signal generation and collection efficiency, and the mechanisms that provide contrast between sub-cellular components. To investigate this parameter space, we have developed a prototype experimental multimodal microscope system (MMS)[22] and determined that wavelengths

Address all correspondence to: Bevin Lin, University of California, Davis, Biomedical Engineering, Shields Drive, Davis, California 95616. Tel: 805 403 8000; E-mail: freddychopin@gmail.com

1083-3668/2011/16(4)/046014/7/$25.00 © 2011 SPIE

shorter than 355 nm penetrate only the superficial layer of cells, resulting in acquisition of high contrast AF images of the epithelial layer of unprocessed tissue specimens (no contrast agents or tissue preparation) using wide-field microscopy.[23,24] It was also found using *ex vivo* human esophageal tissue biopsy specimens under 266-nm excitation resulted in the best image contrast arising mainly from tryptophan emission and its nonuniform distribution within the cells.[25] It was postulated that imaging the epithelial layer with this method would provide more specific histopathologic information related to the disease. Since imaging could be achieved without the use of a signal intensive optical sectioning method (such as confocal or nonlinear excitation), the implementation of high signal throughput image acquisition designs would enable AF microscopic imaging at clinically relevant image acquisition times. Adaptation of this non-contact imaging approach into an endoscope probe for real-time *in vivo* imaging could provide a powerful tool for early detection of epithelial diseases.

The objective of the current research was to explore the possibility of implementing AF endomicroscopy for real-time *in vivo* visualization of epithelial microstructure and organization. We first adapted an image relay lens system for use with a wide-field WL endomicroscope clinical prototype (Olympus Medical Systems Corporation)[26] to explore AF imaging under UV excitation. After evaluating this system, we developed a rigid lens image relay bench-top endomicroscope prototype (BEP) that incorporated solutions to issues identified in our application of the Olympus system. The results helped determine basic design parameters for developing clinical instrumentation, which could provide real-time *in vivo* histopathology information.

2 Materials and Methods

Murine kidney was chosen as the animal model due to the well-defined structure at the microscopic level. Fresh, intact specimens were obtained from animals that were euthanized in a study approved by the University of California, Davis, Animal Use and Care Administrative Advisory Committee.

Human biopsy specimens from patients undergoing routine surveillance for Barrett's esophagus were collected in accordance with a protocol approved by the Institutional Review Board at the University of California, Davis Medical Center. After obtaining the informed consent, endoscopic biopsy specimens from the vicinity of the squamocolumnar junction (Z-line), the gastroesophageal junction, and the proximal stomach (cardia) were obtained from each consented patient. Each specimen was immediately placed in RPMI media (Invitrogen, Carlsbad, California) and transported to the imaging lab where the AF microscopy images were taken. Immediately after completion of the experiments, each tissue biopsy specimen was individually placed in a 10% formalin container for fixation and submitted for histological diagnosis. The evaluation was confirmed by at least two expert pathologists and taken as the diagnostic gold standard from which the optical images were categorized.

3 Experimental Results

3.1 *Experiments and Results Using the Olympus Endo-Cytoscopy System*

A clinical Endo-Cytoscopy System (ECS) prototype (Olympus Medical Systems Corporation, Tokyo, Japan) designed to provide images using the fluorescence of methylene blue[27] and/or narrow-band imaging under WL illumination[28] in contact mode (where the tip of the ECS must be in contact with the tissue) was used to test the AF microscopic imaging approach under UV excitation. The ECS provided image acquisition of a 350 μm $\times$350 μm field of view at a frame rate of 30 Hz, but is not compatible with transmission of UV excitation. For integrating non-contact AF imaging under UV laser excitation into this system without altering existing hardware, a simple image relay approach was adapted to enable off-axis UV laser excitation of the tissue specimen and maintain reasonably high signal collection efficiency. A schematic of this image relay design is depicted in Fig. 1(a).

The image relay system involved a high quality camera lens (Nikon, 28 mm) used to project the image of the tissue surface onto the input of the ECS probe with 1$\times$ magnification. The tip of the ECS probe was secured to a *xyz* stage located directly above a 28-mm camera lens. This is similar to the Hopkins rod-lens relay system,[29] and made it possible to use off-axis UV excitation by providing a working distance of about 3 cm as depicted in Fig. 1. The unprocessed tissue specimen was placed under a quartz cover slip and centered on a sponge in a standard pathology cassette to ensure luminal surface exposure and to maintain tissue moisture during imaging. The cassette was positioned on a second xyz stage directly below the Nikon

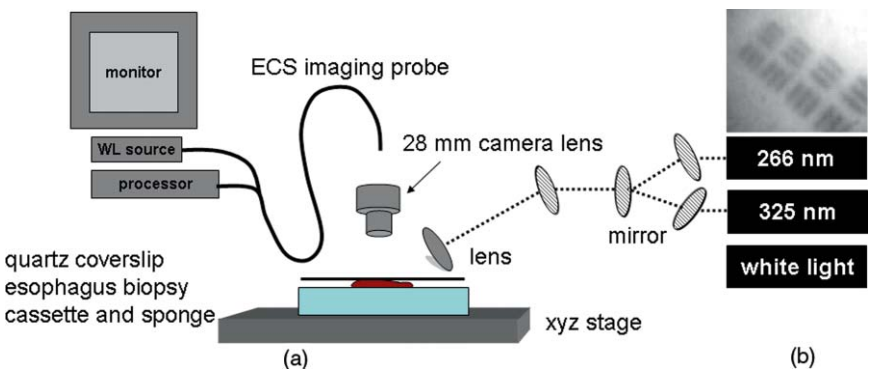

Fig. 1 (a) Schematic diagram of the image relay design used to adapt AF microscopy under 266 and 325 nm excitation into the ECS prototype. Inset (b) shows an image of the resolution target where the line group on the upper left quandrant is 2.2 μm per line.

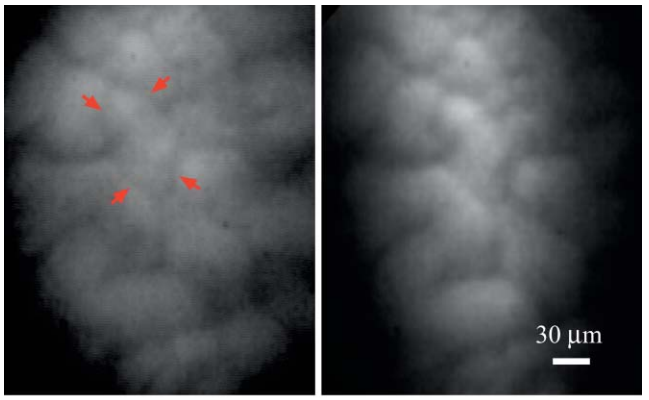

Fig. 2 AF image using the ECS probe of the same region of a murine kidney specimen under (a) 325-nm and (b) 266-nm excitation. Arrows at each of the four quadrants in (a) delineate the outline of an individual tubule.

lens. Using white light and a positive USAF 1951 resolution target (Edmund Optics Inc., Barrington, New Jersey), the spatial resolution of the ECS after relay was estimated to be on the order of 3 to 4 μm as shown in the inset of Fig 1(b).

The output of two compact laser sources, used to excite the tissue specimens in order to acquire the AF images with the ECS, included a 266-nm laser (Intelite, Inc., Minden, Nevada) and a 325-nm laser (Omnichrome, Melles Griot, Carlsbad, California). A converging lens was used to concentrate the excitation laser onto the tissue sample to a beam area of about 3 mm^2, centered at the location of the tissue that was imaged by the ECS. The UV exposure to the tissue surface was about 0.5 mW under 266-nm excitation, and 4 mW under 325-nm excitation.

Figure 2 shows AF endomicroscopy *ex vivo* images in the 410 to 800-nm spectral range (determined by the spectral response of the ECS probe) of the same location from a murine kidney specimen obtained under (a) 325-nm and (b) 266-nm excitation, respectively. The images were acquired without any preparation of the sample beyond removing the capsule to expose the cortex.[30] The outline of a single murine kidney tubule is demarcated using arrows at each of the four quadrants in the image shown in Fig. 2(a) obtained under 325-nm excitation. This same tubule is also visible in the image of the same location shown in Fig. 2(b) that was acquired under 266-nm excitation. These images are similar (considering the lower spatial resolution) to those obtained under 355-nm excitation using our MMS platform. However, although it was expected that the nuclei would be visible under 266-nm excitation as shown in Fig. 6(a) and in previous studies,[23] the image in Fig. 2(b) did not provide the expected nuclei visibility or contrast. It must be noted that the fixed frame rate of the ECS probe at 30 Hz required increased photo-excitation to provide a sufficient AF signal for the detector to record an image. As tryptophan is the main fluorophore contributing to the image formation and contrast under 266-nm excitation, we hypothesized that photobleaching of tryptophan might be responsible for the loss of nuclei visualization. To test this hypothesis, we used the MMS platform to monitor the visualization and contrast of murine kidney cell nuclei as a function of power of the 266-nm laser. We found that increased exposure

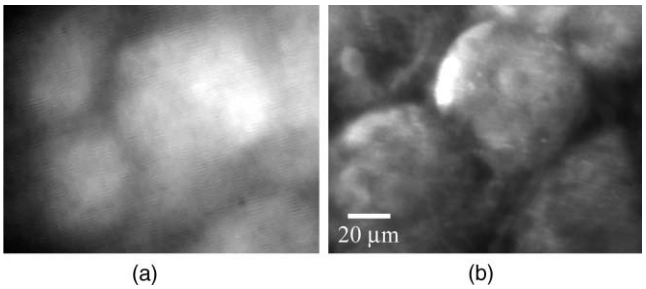

Fig. 3 *Ex vivo* AF images of a human esophageal tissue specimen containing gastric-type mucosa using (a) the Olympus clinical ECS prototype under 325-nm excitation, and (b) the MMS platform under 266-nm excitation.

to 266-nm light leads to loss of nuclei visibility. Experiments to investigate this effect indicated that it arose from photobleaching of tryptophan and was accompanied by a deviation from the linear dependence of AF on the excitation intensity. These results identified a limitation of this approach associated with the photobleaching of tryptophan under prolonged exposure at higher excitation intensities. The simplest way to mitigate this problem in our experiments was to use lower laser power, which in turn would require an image acquisition frame rate lower than 30 Hz (longer image acquisition time).

Understanding these limitations, we used the ECS probe for imaging experiments of human tissue specimens obtained from eight patients. Human esophageal epithelium was imaged with the same approach as the animal tissue, using both 325 and 266 nm laser excitation. The imaging results from two different tissue types are exemplified in Figs. 3 and 4. The esophagus biopsy specimen in Fig. 3 had a pathology diagnosis of gastric-type mucosa. The visible rosette-type features could be expected from a patient with Barrett's esophagus. The largest individual rosette structure in Fig. 3(a) was approximately 75 μm in diameter. This image was acquired using the ECS, and was consistent with the image of the same tissue biopsy specimen acquired using the MMS platform, shown in Fig. 3(b). These gastric-type mucosal features were also visible in the hematoxylin and eosin (H&E) and AF images of human gastric cardia, shown both in Fig. 7 and in preliminary unpublished results.[31]

The biopsy specimen shown in Fig. 4(a) was collected at the Z-line and clearly displays a characteristic honeycomb pattern that could be recognized throughout the ECS image. The corresponding AF image shown in Fig. 4(b) was obtained using the MMS platform. For direct comparison, the image from the H&E stained section obtained using the MMS platform under white light illumination is shown in Fig. 4(c). All three images in Figs. 4(a)–4(c) demonstrated the honeycomb pattern of glandular mucosa under the same magnification, and correlated with previous imaging experiments under 266-nm excitation using the MMS platform.[24]

3.2 *Experiments and Results Using the BEP*

With the experience attained using the ECS probe, we developed a bench-top prototype that addressed the limitations of the current system, but preserved the overall concept for direct translation to a future endomicroscope system. The operational parameters of this prototype system were explored using the

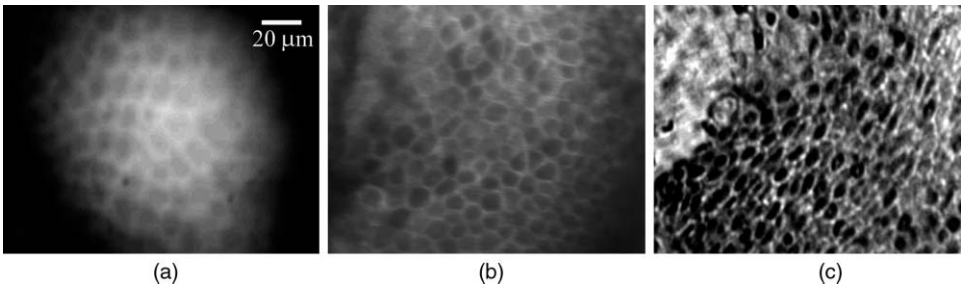

Fig. 4 *Ex vivo* AF images of human esophageal glandular mucosa tissue biopsy specimen under 266-nm excitation using the (a) Olympus clinical ECS prototype, (b) MMS platform, and (c) H&E stained tissue section under white light using the MMS platform, illustrating the typical honeycomb pattern corresponding to (a) and (b).

animal and human tissues. As diagrammed in Fig. 5, the system was secured in a vertical position above a sample holder. To ensure luminal surface exposure and to maintain moisture in the tissue during imaging, the specimens were covered with a quartz cover slip and placed in a standard pathology cassette and sponge. The cassette was positioned directly below a 0.4 numerical aperture ×20 quartz objective, transmitting 266-nm excitation (Thorlabs, Newton, New Jersey) at a working distance of 4 mm. A compact diode-pumped solid state laser operating at 266 nm (Intelite, Inc., Minden, Nevada) was coupled to a UV compatible fiber using a converging lens (L1). The fiber output was then collimated using a second converging lens (L2), and coupled into the microscope's imaging path using a third lens (L3) and a UV dichroic mirror. The defocused image of the fiber output through the microscope objective illuminated an area of about 3 mm^2, centered within the imaged area of the specimen. The AF signal collected by the microscope objective was used to form an image of the illuminated area of the specimen in the input plane of an imaging fiber conduit (Edmund Optics Inc., Barrington, New Jersey). The fiber conduit was 6 inches in length with an outer diameter of 3.2 mm, while the diameter of each individual fiber was 12 μm. These fibers were the effective image pixels when the image was transported through the fiber conduit. This image preserving fiber conduit was not UV compatible and as a result, only the AF signal in the visible range was transmitted to the output side of the conduit. The image at the output side was then projected using an achromat lens (OFR/Thorlabs, Caldwell, New Jersey) onto a thermoelectrically cooled detector (Photometrics, Tucson, Arizona). In this arrangement, each individual fiber of the conduit was projected on approximately 6×6 pixels in the CCD detector. The CCD, lens system, objective, and tissue stage were each mounted on *xyz* stages that enabled rapid alignment and focusing of individual components. The spatial resolution of the BEP system was better than 2.2 μm, as determined from the image of a positive USAF 1951 resolution target (see the inset of Fig 5). Imaging of tissue specimens was performed using 4×4 pixel binning without significant loss of image resolution, which is determined by the projected size of the individual fibers of the conduit (6×6 pixels). The tissue was exposed to a laser power of about 500 μW for an *ex vivo* dose of 8 mJ/cm^2. Images were acquired under 0.5 second exposure, which yielded a digitized intensity of about 3000 counts per pixel.

Figure 6 demonstrated two separate intact murine kidney specimens under 266-nm excitation. The image in Fig. 6(a) was acquired using the MMS platform and contained several tubules. The boundary between two individual tubules is partially outlined for visual aide. A dark feature believed to be a cell nucleus is indicated at the tip of the arrow within the tubule itself. These tubular outlines and dark nuclei were visible throughout the tissue surface and were comparable to the same features acquired with the BEP system, shown in Fig. 6(b). It should be noted that the scale bar indicates the approximate radius of individual tubules, and the overall surface diameter is on the order of 30 μm.

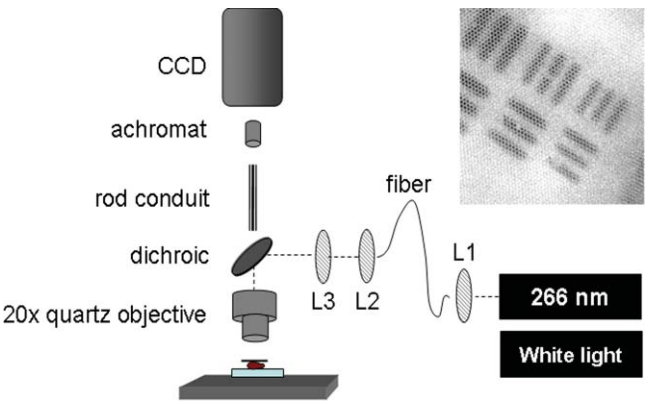

Fig. 5 Schematic diagram of the BEP rod conduit image relay system. Inset shows an image of the resolution target where the line group of 2.2 μm per line is on the lower right quandrant.

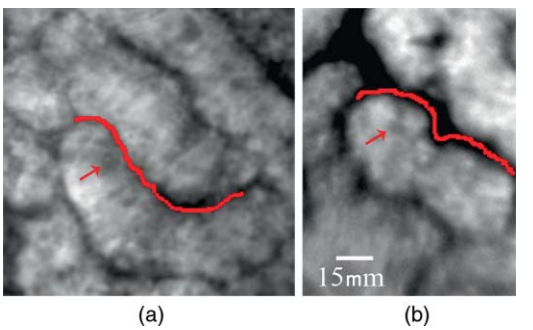

Fig. 6 AF images of two fresh intact rat kidney specimens under 266-nm excitation using the (a) MMS platform, and (b) the BEP system. Individual tubules and nuclei (example shown with outlines and arrows) are visible in each image.

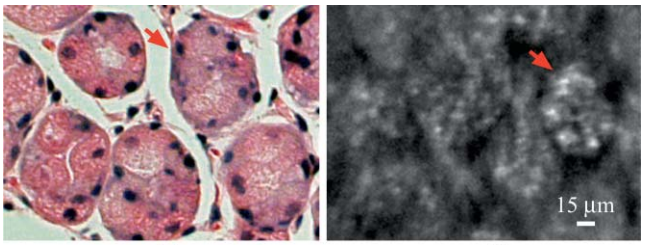

Fig. 7 A single human gastric epithelium biopsy specimen (a) using the H&E slide specially sectioned parallel to the mucosal surface (as opposed to the cross section), and (b) the corresponding mucosal surface optical image from the BEP system under 266-nm exposure. Rosette-like features, indicated with an arrow, can be appreciated in both images. The field of view is 225 μ×168 μm.

Human gastric cardia specimens from a total of 6 patients were imaged with the BEP system using 266-nm laser excitation. A typical AF image example is shown in Fig. 7(b). For comparison, a specially surface-sectioned H&E slide of the same specimen, shown in Fig. 7(a), was prepared parallel to the mucosal surface (as opposed to the traditional cross-section) to achieve the same projection as the AF image. The arrow indicates a single rosette-type structure of the gastric tissue in both the H&E image and the AF image. These features are similar to the gastric-type esophageal cells shown in Fig. 3.

4 Discussion

The experimental results demonstrate proof of principle that wide-field endomicroscopy using tissue AF under UV excitation is technically feasible. The ECS clinical prototype provided cellular resolution of murine kidney tubules (Fig. 2) as well as human esophageal gastric-type and glandular mucosa (Figs. 3 and 4) without contrast agents. Furthermore, higher quality images were obtained using the BEP system, as shown in Figs. 6(b) and 7(b).

The *ex vivo* AF images obtained using the BEP system were acquired under an approximate dose of 8 mJ/cm^2, which is above the ANSI defined 3 mJ/cm^2 maximum permissible exposure (MPE) for dosage to UV wavelengths between 180 and 302 nm.[32] This hazard classification was based on ocular damage, the standard reference for *in vivo* tissue MPE. There are multiple improvements in the system's components that can reduce the current *ex vivo* dosage by more than 1 order of magnitude for future *in vivo* implementation. Most important is the appropriate selection of the image transporting optical element, which in our case was the image preserving fiber conduit. This fiber conduit only transmitted the emission at wavelengths longer than about 400 nm. Therefore, as the AF signal under 266-nm excitation is mostly due to tryptophan emission centered in the 320 to 350 nm spectral region,[25] only a small portion of this signal (on the order of 10%) was transmitted through the fiber conduit. Using a UV compatible image transporting element would increase the signal available to be detected by the CCD detector by about 1 order of magnitude. Furthermore, the CCD detector used for image acquisition had only about 30% quantum efficiency (QE) between 400 and 450 nm (which covered the spectral range where most of the detected signal was located). Therefore, appropriate selection of the CCD detector to provide optimized sensitivity in the 300 to 500 nm spectral range could enhance the signal detection efficiency by another factor of 2. Finally, we found that decreasing the overall image intensity count to 1/4 of that used (currently with pixel intensity of 3000 counts) during the experiments did not produce a significant deterioration of the image quality. That is, it would not be possible for an observer in a clinical setting to distinguish images of 3000 counts per pixel from 800 counts per pixel based on visual perception of image quality. Hence, only these three improvements discussed above could lead to reduction in the required exposure dosage by close to a factor of 100 from the current dose of 8 mJ/cm^2 used in our experiments (or about 40× below the ANSI defined MPE of 3 mJ/cm^2).

The small (225 μm×168 μm) field of view (FOV) of the BEP system was due to the limited number of fibers of the image transport conduit. In order to achieve spatial resolution on the order of 1 μm, the magnification in the front end of the system was adjusted so that an area of about 1 μm^2 at the tissue plane was projected into a single fiber at the input of the fiber conduit. By using a different image transport system, it is possible to increase the FOV without loss of spatial resolution. For example, using an image transport system that preserved the spatial resolution at the input plane (such as a near-UV optimized rod lens system), the FOV can be increased to more than 1 mm^2 (determined by the number of pixels and the pixel size of the CCD camera). This in turn would greatly enhance the ability to screen larger tissue areas within a clinically relevant time frame compared to the current scanning confocal systems.

The elimination of contrast agents will arguably improve safety, cost, and time efficiency. Current surveillance guidelines during upper endoscopy procedures collect random four quadrant biopsies every one to two centimeters throughout the length of glandular epithelium in Barrett's esophagus. The pathology cost alone for each biopsy collected is substantial and increases as additional tissue biopsy specimens are collected and sent for diagnosis. Thus, a technology that could reliably identify cellular level changes indicative of a premalignant state enables targeted biopsies and has the potential to dramatically reduce the number and cost of random biopsies.[8,33] Integration of an endomicroscopy technique such as the method discussed in this work with conventional endoscopy to determine the regions of interest for directed biopsy and/or optical biopsy might be the most efficient approach in terms of technical feasibility and integration of information provided by novel technology with current state-of-the-art clinical practice. Optical capabilities and parameters of our current BEP could be easily implemented into endoscopic embodiments to provide real-time *in vivo* diagnostic information.

The results also indicated that a sufficient contrast and spatial resolution necessary to distinguish morphological cellular changes were obtained using the system. These changes included rosette features of the esophagus and cardia, shown in Figs. 3 and 7(b), and the distinct honeycomb pattern of esophageal glandular mucosa in Fig. 4. Experimental results of human esophageal mucosal biopsy specimens[25] suggested that the mechanism behind the high contrast imaging of the epithelial layer using wide-field microscopy designs was due to the selected short excitation wavelengths, which only propagated through the tissue to about 50 μm, the approximate penetration depth of UV excitation light. As a result, a

sufficient amount of the AF signal produced in the superficial tissue layer could be contained within the microscope's depth of field, sufficiently reducing the out-of-focus signal to allow the formation of high contrast images without the need to use spatial filtering. We are currently working on the development of guidelines for interpreting the AF images obtained from a wide variety of pathological conditions to provide rules of interpretation for enabling *in vivo* optical histopathologic evaluation.[31]

A future system would ideally incorporate both macro- and micro-imaging capabilities to first survey a large surface area at the tissue level, followed by a smooth transition to the cellular level via a zoom lens. Mapping capabilities would enable more direct correlation between optical and histopathological recognition. Additionally, the sensitivity and specificity for premalignant conditions such as dysplasia must be substantiated. Deformable liquid optics may be a key part of such future designs.

Pulsed illumination may be another method of optimizing AF imaging while better controlling the delivery of the laser energy to the tissue and eliminating motion artifacts. *In vivo* imaging can be plagued with motion artifacts due to intrinsic micro- and macro- vasculature and musculature movements such as circulation and breathing that could ultimately limit *in vivo* application.[34] Thus, the image quality of an *in vivo* microscope system depends not only on the design characteristics of the optical components, but also the degree to which the object being imaged can be kept immobilized with respect to the imaging system during image acquisition. Taking into account that the emission lifetime of the tissue chromophores is on the order of 10 nsec, the overall time-frame needed for image acquisition could be approximately 20 nsec. Therefore, pulsed excitation would not only enable better control over the amount of light delivered to a specific location, but also enable image acquisition much faster than the tissue can move beyond the spatial resolution relative to the imaging system. In addition, an uncooled CCD (or other type of array detector) could be used to capture the images without thermal noise problems typically associated with prolonged acquisition times. This is also important for the miniaturization of the instrument such as placing the CCD detector at the tip of an endoscope.

Acknowledgments

We thank Dr. Kazuhiro Gono, Dr. Takeshi Ozawa, and Dr. Nobuyuki Doguchi of Olympus Medical Systems Corp. for lending us the Endo-Cytoscopy System. We also thank Chris Pivetti for supplying murine kidney specimens. This work was performed in part under the auspices of the U.S. Department of Energy by Lawrence Livermore National Laboratory under Contract No. DE-AC52–07NA27344. This research was supported by funding from the Center for Biophotonics, an NSF Science and Technology Center, managed by the University of California, Davis, under Cooperative Agreement No. PHY 0120999.

References

1. B. Young and J. W. Heath, *Wheater's Functional Histology*, Elsevier Limited, Philadelphia (2000).
2. A. Das, M. V. Sivak, A. Chak, R. C. K. Wong, V. Westphal, A. M. Rollins, J. Willis, G. Isenberg, and J. A. Izatt, "High-resolution endoscopic imaging of the GI tract: a comparative study of optical coherence tomography versus high-frequency catheter probe EUS," *Gastrointest. Endosc.* **54**(2), 219–224 (2001).
3. J. A. Evans, J. M. Poneros, B. E. Bouma, J. Bressner, E. F. Halpern, M. Shishkov, G. Y. Lauwers, M. Mino-Kenudson, N. S. Nishioka, and G. J. Tearney, "Optical coherence tomography to identify intramucosal carcinoma and high-grade dysplasia in Barrett's esophagus," *Nat. Clin. Pract. Gastroenterol. Hepatol.* **4**(1), 38–43 (2006).
4. R. Davila, "Chromoendoscopy," *Gastroenterol. Clin. North Am.* **19**(2), 193–208 (2009).
5. K. Sasajima, S. Kudo, H. Inoue, T. Takeuchi, H. Kashida, E. Hidaka, H. Kawachi, M. Sakashita, J. Tanaka, and A. Shiokawa, "Real-time in vivo virtual histology of colorectal lesions when using the endocytoscopy system," *Gastrointest. Endosc.* **63**(7), 1010–1017 (2006).
6. T. Muldoon, S. Anandasabapathy, D. Maru, and R. Richards-Kortum, "High-resolution imaging in Barrett's esophagus: a novel, low-cost endoscopic microscope," *Gastrointest. Endosc.* **68**(4), 737–744 (2008).
7. S. Kantsevoy, D. Adler, J. Conway, D. Diehl, F. Farraye, V. Kaul, S. Kethu, R. Kwon, P. Mamula, and S. Rodriguez, "Confocal laser endomicroscopy," *Gastrointest. Endosc.* **70**(2), 197–200 (2009).
8. M. Wallace and P. Fockens, "Probe-based confocal laser endomicroscopy," *Gastroenterology* **136**(5), 1509–1513 (2009).
9. K. B. Dunbar, P. Okolo III, E. Montgomery, and M. I. Canto, "Confocal laser endomicroscopy in Barrett's esophagus and endoscopically inapparent Barrett's neoplasia: a prospective, randomized, double-blind, controlled, crossover trial," *Gastrointest. Endosc.* **70**(4), 645–654 (2009).
10. C. Gheorghe, R. Iacob, G. Becheanu, and M. Dumbrava, "Confocal endomicroscopy for in vivo microscopic analysis of upper gastrointestinal tract premalignant and malignant lesions," *J. Gastrointestin. Liver Dis.* **17**(1), 95–100 (2008).
11. M. Wallace, "Leeuwenhoek meets kussmaul: The evolution of endoscopist to endo-pathologist," *Gastroenterology* **131**(2), 347–349 (2006).
12. A. Meining, "Confocal Endomicroscopy," *Gastrointest. Endosc. Clin. N. Am.* **19**(4), 629–635 (2009).
13. T. D. Wang, S. Friedland, P. Sahbaie, R. Soetikno, P. L. Hsiung, J. T. C. Liu, J. M. Crawford, and C. H. Contag, "Functional imaging of colonic mucosa with a fibered Confocal microscope for real-time in vivo pathology," *Nat. Clin. Pract. Gastroenterol. Hepatol.* **5**(11), 1300–1305 (2007).
14. M. Wallace, A. Meining, S. Miehlke, T. Rosch, H. Pohl, C. Lightdale, B. Filoche, D. Carr-Locke, E. Coron, and J. Moreau, "Safety of intravenous fluorescein for probe-based confocal laser endomicroscopy (pCLE): A multicenter study," *Gastrointest. Endosc.* **69**(5), AB367–AB368 (2009).
15. R. Kester, T. Tkaczyk, M. Descour, T. Christenson, and R. Richards-Kortum, "High numerical aperture microendoscope objective for a fiber confocal reflectance microscope," *Opt. Express* **15**(5), 2409–2420 (2007).
16. M. Nakao, S. Yoshida, S. Tanaka, Y. Takemura, S. Oka, M. Yoshihara, and K. Chayama, "Optical biopsy of early gastroesophageal cancer by catheter-based reflectance-type laser-scanning confocal microscopy," *J. Biomed. Opt.* **13**(5), 054043 (2008).
17. H. Shin, M. Pierce, D. Lee, H. Ra, O. Solgaard, and R. Richards-Kortum, "Fiber-optic confocal microscope using a MEMS scanner and miniature objective lens," *Opt. Express* **15**(15), 9113–9122 (2007).
18. D. Li, W. Zheng, and J. Qu, "Imaging of epithelial tissue in vivo based on excitation of multiple endogenous nonlinear optical signals," *Opt. Lett.* **34**(18), 2853–2855 (2009).
19. W. Rice, D. Kaplan, and I. Georgakoudi, "Quantitative biomarkers of stem cell differentiation based on intrinsic two-photon excited fluorescence," *J. Biomed. Opt.* **12** 060504 (2007).
20. G. K. Anagnostopoulos, K. Yao, P. Kaye, C. J. Hawkey, and K. Ragunath, "Novel endoscopic observation in Barrett's oesophagus using high resolution magnification endoscopy and narrow band imaging," *Aliment. Pharmacol. Ther* **26**(3), 501–507 (2007).
21. W. L. Curvers, R. Singh, L. M. W. K. Song, H. C. Wolfsen, K. Ragunath, K. Wang, M. B. Wallace, P. Fockens, and J. J. G. H. M. Bergman, "Endoscopic tri-modal imaging for detection of early neoplasia in Barrett's oesophagus: a multi-centre feasibility study using high-resolution endoscopy, autofluorescence imaging and narrow band imaging incorporated in one endoscopy system," *Gut* **57**(2), 167–172 (2008).

22. S. G. Demos, C. A. Lieber, B. Lin, and R. Ramsamooj, "Imaging of tissue microstructures using a multimodal microscope design," *IEEE J. Sel. Top. Quant. Electron.* **11**(4), 752–758 (2005).
23. B. Lin, C. A. Lieber, J. T. Fitzgerald, A. P. Michalopoulou, R. N. Raman, C. D. Pivetti, C. Troppmann, D. L. Matthews, and S. G. Demos, "Real-time Imaging of tissue microstructures using intrinsic optical signatures," in *SPIE Photonics West BiOS Optical Biopsy VI*, A. K. Robert, R. Alfano, Eds., San Jose, CA (2006).
24. B. Lin, S. Urayama, R. M. G. Saroufeem, D. L. Matthews, and S. G. Demos, "Real-Time Microscopic imaging of esophageal epithelial disease with autofluorescence under ultraviolet excitation," *Opt. Express* **17**(15), 12502–12509 (2009).
25. B. Lin, S. Urayama, R. Saroufeem, D. Matthews, and S. Demos, "Characterizing the origin of autofluorescence in human esophageal epithelium under ultraviolet excitation," *Opt. Express* **18**(20), 21074–21082 (2010).
26. K. Gono, "Multifunctional endoscopic imaging system for support of early cancer diagnosis," *IEEE J. Sel. Top. Quant Electron.* **14**(1), 62–69 (2008).
27. Y. Kumagai, K. Monma, and K. Kawada, "Magnifying chromoendoscopy of the esophagus: in-vivo pathological diagnosis using an endocytoscopy system," *Endoscopy* **36**(7), 590–594 (2004).
28. K. Gono, T. Obi, M. Yamaguchi, N. Ohyama, H. Machida, Y. Sano, S. Yoshida, Y. Hamamoto, and T. Endo, "Appearance of enhanced tissue features in narrow-band endoscopic imaging," *J. Biomed. Opt.* **9**, 568–577 (2004).
29. S. J. Dobson and H. H. Hopkins, "A new rod-lens relay system offering improved image quality," *J. Phys. E* **22**(7), 450–455 (1989).
30. R. Raman, C. Pivetti, A. Rubenchik, D. Matthews, C. Troppmann, and S. Demos, "Evaluation of the contribution of the renal capsule and cortex to kidney autofluorescence intensity under ultraviolet excitation," *J. Biomed. Opt.* **14**, 020505 (2009).
31. B. Lin, S. Urayama, R. M. G. Saroufeem, D. L. Matthews, and S. G. Demos, "Early identification and establishment of rules for interpretation of endoscopically invisible intestinal metaplasia using ultraviolet autofluorescence for real-time histology," (*in preparation*).
32. "American National Standards Institute for Safe Use of Lasers Z136.1" (2000).
33. J. Inadomi, R. Sampliner, J. Lagergren, D. Lieberman, A. Fendrick, and N. Vakil, "Screening and surveillance for Barrett esophagus in high-risk groups: a cost-utility analysis," *Ann. Intern. Med.* **138**(3), 176–186 (2003).
34. H. C. Wolfsen, "New technologies for imaging of Barrett's esophagus," *Surg. Oncol. Clin. N. Am.* **18**(3), 487–502 (2009).